UCRL- 97547
PREPRINT

The Role of Low Temperature Chemistry in the Autoignition of N-Butane

R. M. Green
Sandia National Laboratories

N. P. Cernansky
Drexel University

W. J. Pitz and C. K. Westbrook
Lawrence Livermore National Laboratory

1987 SAE International Fuels and Lubricants
Meeting and Exposition
Toronto, Ontario
November 2-5, 1987

Lawrence Livermore National Laboratory

This is a preprint of a paper intended for publication in a journal or proceedings. Since changes may be made before publication, this preprint is made available with the understanding that it will not be cited or reproduced without the permission of the author.

CIRCULATION COPY
SUBJECT TO RECALL
IN TWO WEEKS

DISCLAIMER

This document was prepared as an account of work sponsored by an agency of the United States Government. Neither the United States Government nor the University of California nor any of their employees, makes any warranty, express or implied, or assumes any legal liability or responsibility for the accuracy, completeness, or usefulness of any information, apparatus, product, or process disclosed, or represents that its use would not infringe privately owned rights. Reference herein to any specific commercial products, process, or service by trade name, trademark, manufacturer, or otherwise, does not necessarily constitute or imply its endorsement, recommendation, or favoring by the United States Government or the University of California. The views and opinions of authors expressed herein do not necessarily state or reflect those of the United States Government or the University of California, and shall not be used for advertising or product endorsement purposes.

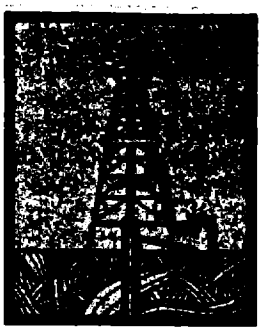

1987 SAE International Fuels and Lubricants Meeting & Exposition

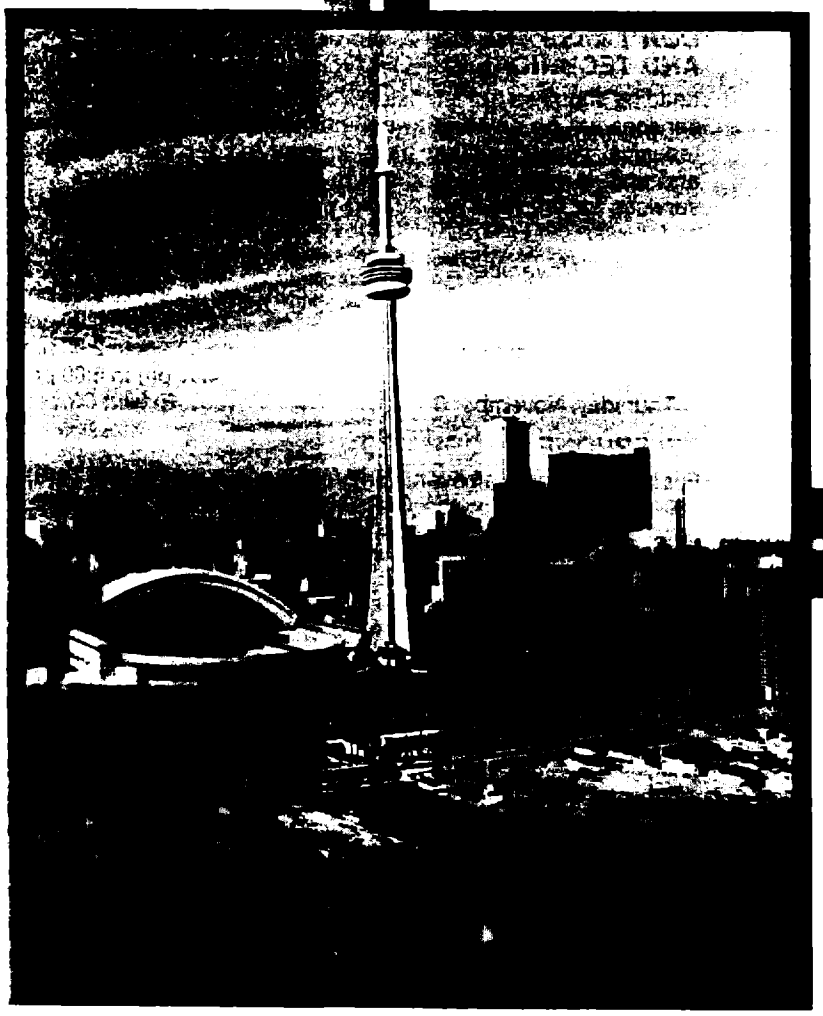

November 2-5, 1987
Toronto Harbour Castle
Hilton Hotel and Convention Center
Toronto, Ontario

ABSTRACT

We have studied the chemical aspects of the compression ignition of n-butane experimentally in a spark ignition engine and theoretically using computer simulations with a detailed chemical kinetic mechanism. The results of these studies demonstrate the effect of initial charge composition on autoignition. Experimentally, when the initial charge consisted of 80% fresh charge and 20% recycled products of combustion, we observed that autoignition was inhibited. On the other hand, charging with 80% fresh charge and 20% partial oxidation products from the previous motored cycle resulted in enhanced low-temperature chemistry (with the associated heat release and temperature increase) and autoignition. We assessed how well the detailed kinetic model could predict the autoignition and modified the model to better simulate the experimental observations. We also assessed how chemical preconditioning of the fuel-air charge affected the autoignition process.

OVER THE YEARS, studies of knock in spark ignition engines have included nearly all aspects of engine combustion. Investigations involving experiments and/or modeling have probed the chemical, thermodynamic, and mechanical details of the processes involved and have resulted in significant advances in our understanding of what occurs prior to autoignition and knock [1].* Unfortunately, there are still many facets of the problem that we need to unravel in order to control engine knock. In this regard, it is necessary to improve our current understanding of the end-gas autoignition processes that can lead to engine knock.

There are three general classes of problems associated with end-gas autoignition: (1) fluid motion and heat transfer, (2) cylinder wall deposits, and (3) the ignition chemistry of the fuel. Our work has focused on the ignition chemistry because it tends to be relatively independent of specific engine design, and because it is a common factor in all aspects of the knock process and can be readily isolated from the other important phenomena. Overall, our goal has been to improve our understanding of the low temperature chemistry occurring in the compressively-heated end gas prior to autoignition and knock.

Our work has involved both engine related studies and parallel detailed chemical kinetic modeling studies [2]. The engine studies have included laser diagnostics and physical sampling of the end gas. During the course of the experimental work, we noticed some interesting and unique engine operating conditions when the engine was only fired with the spark ignition every third cycle. Here we attained an operating condition where the first cycle after the fired cycle was a normal skip (or motored) cycle and the second cycle after the fired cycle compressively ignited by autoignition. Such behavior has significant implications relative to the effects of charge preconditioning and exhaust product recycling on end-gas autoignition and engine knock. This paper reports an experimental and modeling study undertaken to explore this behavior.

BACKGROUND

End-gas chemistry has been studied for many years. Major contributions have been made by Egerton et al. [3], Downs et al. [4,5], Pahnke et al. [6], Walcutt et al. [7], Sturgis [8], Gluckstein and Walcutt [9], Johnson et al. [10], Halstead et al. [11] and others. This work was recently reviewed by Green et al. [1] who pointed out several common threads that seem to connect these studies. In particular, there appears to be some question as to the importance of the preknock reactions occurring in the end gas. While some research indicates that these reactions are necessary to precon-

* Numbers in brackets designate references at end of paper.

dition the fuel-air mixture for the autoignition to occur, others seem to indicate that the specific nature of these reactions is really unimportant; they argue that the effects of antiknock additives are limited only to the high temperature ignition reactions and not to the low-temperature preknock reactions. Also, nearly all of the work suggests that there is a reasonable amount of heat released due to the preknock reactions. Finally, where temperature measurements were made (Gluckstein and Walcutt [9] and Johnson et al. [10]), it was evident that the heat released by the preknock reactions was sufficient to affect the end-gas temperatures significantly, and that this was an important process leading to autoignition and knock.

More recently, several investigators have examined ignition phenomena in a variety of experimental systems. Najt and Foster [12] studied compression ignition of homogeneous fuel-air mixtures in an engine system. They concluded that the ignition process is controlled by low temperature (below $950K$) hydrocarbon oxidation kinetics. Griffiths and coworkers [13,14] looked at spontaneous ignition in a rapid compression machine. They reported that "low temperature" degenerate chain branching controls the preignition heat release and that the negative temperature-coefficient-of-reaction behavior of the fuel can be significant in the autoignition event. Wilk et al. [15,16] concluded from their static reactor experiments that low and intermediate temperature chemistry (below $650K$ and $650 - 900K$, respectively) is significant in the autoignition event. Lignola and co-workers [17,18] observed spontaneous ignition and cool flame behavior in a continuously stirred tank reactor. They concluded that knocking is a "thermokinetic" event with kinetics playing a major role.

A number of investigators have developed theoretical models for the autoignition of hydrocarbon fuels at conditions related to engine knock. Halstead et al. [11] developed the "Shell Model" which employs a multistep, global kinetic mechanism to treat the autoignition of primary reference fuels. Their global mechanism has been adjusted to predict the measured autoignition time. The "Shell Model" is well-suited for use in multidimensional models of engine knock [19]. Keck and Hu [20] also developed a simplified, global kinetic model for the autoignition of hydrocarbons at low and intermediate temperatures. They have compared the results of their model to experimental results in a constant volume bomb. A series of detailed chemical kinetic modeling studies have investigated the autoignition of n-butane and isobutane [1,2,21,22]. The results of these studies showed the importance of reactions involving the HO_2 radical at the high pressure conditions found in engines. Leppard [23] investigated the autoignition of ethane-air mixtures using the detailed kinetic mechanism of Westbrook and Dryer [24].

It seems apparent that a comprehensive understanding of autoignition and knock must identify the relative importance of the preknock reactions acting as a chemical preconditioning of the fuel-air mixture and as a source of heat release that raises the temperature of the end gas. The significance of the preknock, end-gas reactions in preparing the fuel-air mixture for autoignition must be evaluated. In this regard, the application of advanced laser diagnostic tools for the determination of the end-gas temperatures, the use of modern sampling and analytical techniques for determining mixture compositions, and the use of large, high-speed computers to integrate the many rate equations of the complex chemical kinetic mechanisms needed to model autoignition reactions currently provides analysis techniques not available to previous researchers. Thus, appropriate utilization of these tools, with guidance from the pioneering and more recent work noted above, should enable improvements in our understanding of the end-gas autoignition process.

In an attempt to meet this challenge, we are currently pursuing a research program that emphasizes the low-temperature chemistry occurring in compressively heated end gas [1,2]. This effort is comprised of parallel experimental and modeling studies aimed at developing comprehensive chemical kinetic mechanisms that can model the oxidative breakdown of the fuel and the autoignition of the end gas. We recognize that the chemical phenomena represent only a portion of the processes occurring in the end gas prior to autoignition. However, since this class of processes is generic rather than tied to specific engine design, and can be easily isolated for detailed study, we have chosen to concentrate our efforts in this area.

In general, our experimental work is based on controllable, repeatable knocking operation in our optical research engine [1,2,25]. With a recently implemented thermodynamic heat release analysis [26], we can estimate the temperature history of the end-gas (the adiabatic core) from the measured combustion chamber pressure history, up to the point of sensible energy release in the end gas which is not included in the model. We have verified the adequacy of this analysis using nonperturbing laser diagnostic techniques [26,27,28]. Using a fast-acting gas sampling valve to obtain time-resolved samples of end gas prior to the autoignition and using gas chromatography to analyze these samples, we can determine the concentration histories of the stable species present in the end gas [22]. The temperature and pressure histories are used as inputs to detailed chemical kinetic simulations of the end-gas chemistry. The results of these calculations are compared with the measured species concentration histories to verify the adequacy of the models. The calculated times-of-autoignition can be compared with the measured values and provide further evidence as to the validity of the kinetic models. Ultimately, we hope that the models can be used to predict accurately the occurrence of autoignition from a given end-gas temperature and pressure history.

EXPERIMENT DESCRIPTION

We carried out our experimental work using the

Sandia optical research engine, firing the engine every third cycle. The cylinder head of this engine was configured with a cylindrical combustion chamber yielding a 5.1 compression ratio, four spark plugs equally spaced around its perimeter, and a shrouded intake valve to produce a highly swirling intake flow. The simultaneous firing of the four spark plugs on firing cycles resulted in a flame propagation dominated by swirl-induced convection, with the end gas confined to the center of the combustion chamber. Since only small portions of the piston dome and chamber top contact the end gas, heat transfer and surface chemistry were limited. This configuration, along with the high turbulence level in this engine, resulted in a very homogeneous condition in the end gas and, when autoignition occurred, a nearly simultaneous autoignition throughout the whole end-gas region. Under normal operation, the manifold temperature and pressure were used to control the fraction of fuel-air mixture that autoignited and the skip-fire strategy significantly reduced the cycle-to-cycle variations resulting from a large residual fraction. This experimental configuration allowed us easily to maintain stable and repeatable engine operation.

We measured the combustion chamber pressure histories to determine the time of autoignition and to estimate the end-gas temperature history. Species concentration measurements were made using a fast-acting sampling valve, a sample collection and holding system, and a gas chromatograph (GC) operating with a flame ionization detector (FID) for the analysis of the samples. Details of the engine instrumentation and general operating procedures are presented elsewhere [1].

For the current experiments, the engine control parameters were tuned to achieve the unique stable operating mode described above. In particular, we had a normal fired cycle resulting in end-gas autoignition and knock, followed by a normal skip cycle without autoignition, followed by a skip cycle which autoignited. Since the normal scavenging efficiency of the engine is roughly 80%, these cycles contained 80% fresh charge and either 20% recycled products of combustion (in the case of a prior fired or autoigniting cycle) or 20% recycled, partially-oxidized reactants (in the case of a prior skip cycle). All experiments were conducted at an equivalence ratio of 0.85, with a 352 crankangle degrees (CAD) spark timing on the fired cycle. Engine speeds of 300 and 600 rpm were examined, with inlet manifold conditions of 162C, 1.64 bars and 155C, 1.77 bars, respectively. For the skip cycle, gas samples were collected during both the compression and expansion strokes, while for the fired and compression ignition cycles, samples were obtained only up to the time of autoignition.

EXPERIMENTAL RESULTS

END-GAS PRESSURE AND TEMPERATURE - The basic behavior observed in these experiments is illustrated in Fig. 1, which presents single cycle pressure histories, covering the time from late in the compression stroke to well into the expansion stroke, for the three types of engine cycles. In the fired cycle, one can observe

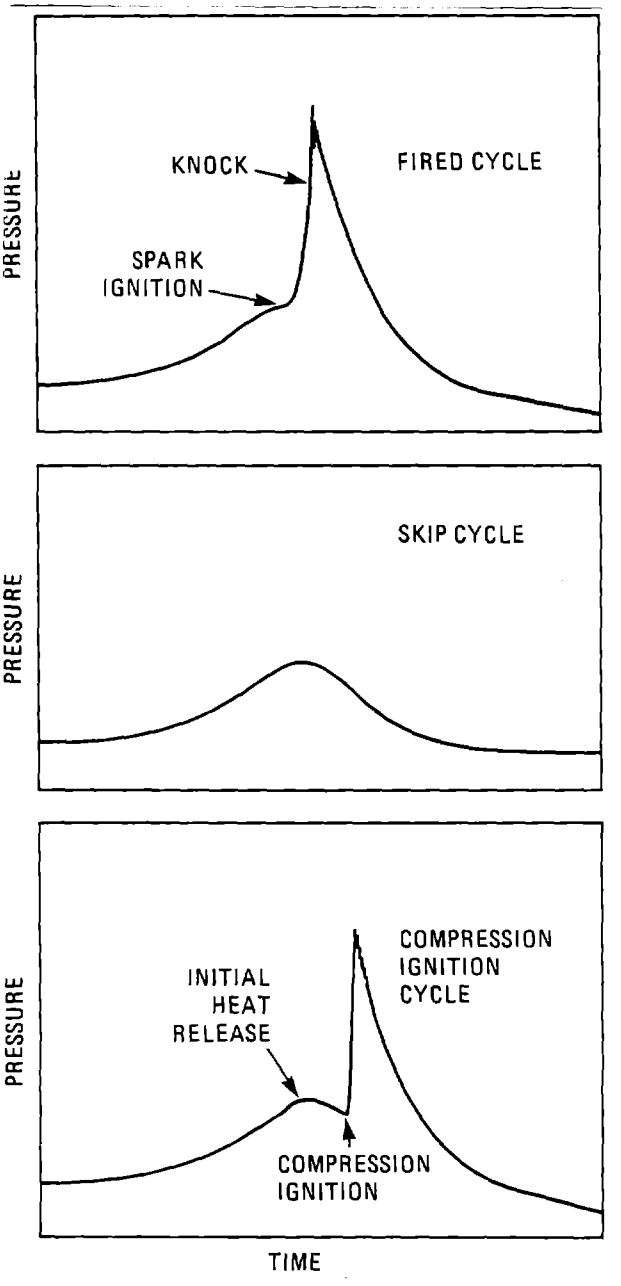

Figure 1. Typical pressure histories illustrating the compression and expansion strokes of the fired, skip and compression ignition cycles for an engine speed of 600 rpm. Notice that the heat release near TDC in the compression ignition cycle, is not present in the fired or the skip cycles.

the discontinuity in the rate of heat release that occurs at the autoignition point, the high rate of heat release after autoignition, and the characteristic pressure oscillations that accompany knocking operation. For the first skip cycle, there is a barely perceptible heat release prior to TDC due to preignition reactions and there is no hot ignition. On the other hand, the second skip cycle shows a noticeable degree of preignition-reaction heat release before TDC and has a clearly defined autoignition event well after TDC.

In Fig. 2(a) we have overlayed the pressure history for a cycle on which compression ignition occurred with that from the motored (skip) cycle immediately preceeding it. The overlay of these pressure histories clearly illustrates the two-stage character of the ignition process. For comparison, we have included in Fig. 2(b) a sketch of the typical ignition event observed in rapid compression machines (see, for example, Taylor et al. [29] or Halstead et al. [11]). Notice the strong similarity in the ignition pressure histories from the two types of experiments. Clearly, in the present experiments, we are investigating the same chemical processes that have been under investigation for several decades.

The pressure histories measured near the time of autoignition, and the temperature histories calculated using the thermodynamic model are illustrated in Figs. 3 and 4. These quantities are plotted as a function of crankangle at two engine speeds for each type of engine cycle. Multiple data sets are included to illustrate system reproducibility; the symbols in the fired cycle cases indicate the values of these quantities at the measured knock point.

Consider the effect of engine speed on the measured pressures and calculated temperatures. For the fired cycles, the calculated end-gas temperature during the later stages of compression and heat release, as well as at the knock point, increases with engine speed. During compression, but prior to spark ignition, this effect is probably due to heat transfer and blowby, which are strongly dependent on engine speed. This explanation is supported by the pressure data which show that before spark ignition on the fired cycle and/or prior to heat release in the skip and compression ignition cycles, the pressure measured at 300 rpm is somewhat lower than that measured at 600 rpm. This difference carries directly into the temperature calculations and accounts for the difference observed above. However, during flame propagation and including the knock point, the effect of heat release in the end gas can become significant, resulting in the thermodynamic model underpredicting the end-gas temperature. This factor will be more important at lower engine speeds where there is more time for the low-temperature chemistry to proceed and produce a larger amount of heat release in the end-gas. There is also direct experimental confirmation of this effect as can be seen in Figs. 3 and 4. For the compression ignition cycles, there is a considerable amount of heat release occurring simply due to the preflame reactions and, at the lower engine speed where more time is available, considerably more heat release occurs near the top dead center position with autoignition occurring sooner.

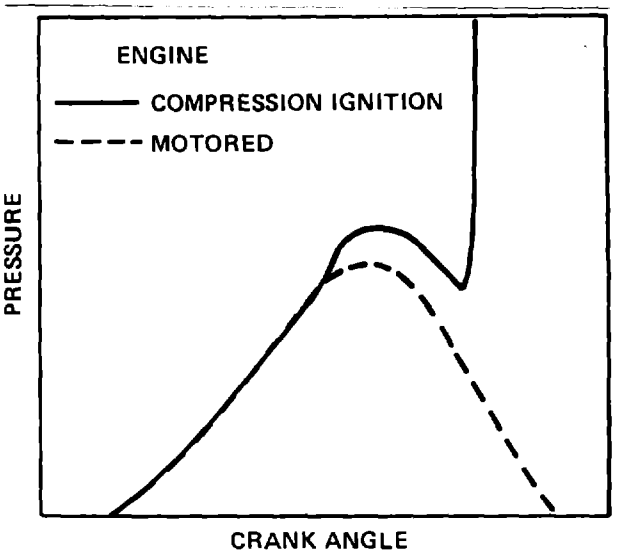

Figure 2(a). Overlayed pressure histories from a compression ignition cycle and the preceding motored cycle illustrating the two-stage characteristic of the ignition process.

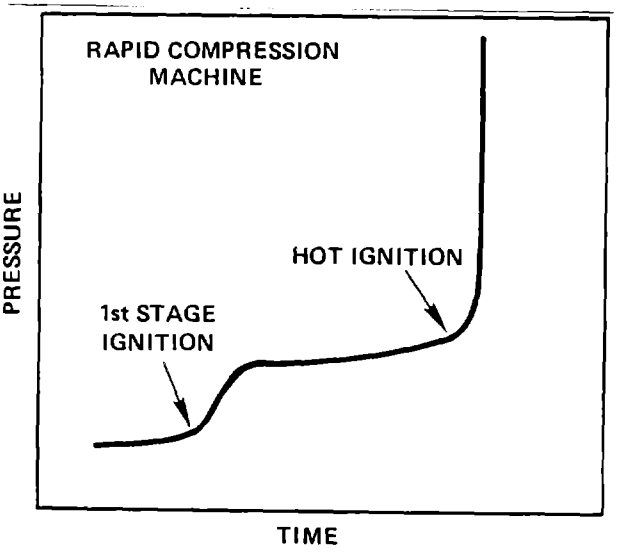

Figure 2(b). The pressure history observed during a typical ignition event in a rapid compression machine illustrating the nature of that ignition process.

END-GAS SAMPLING RESULTS - We carried out cycle-averaged sampling and GC analysis for each of the three types of engine cycles at both of the engine operating conditions. The chromatogram shown in Fig. 5 illustrates a typical result of the gas composition analysis and indicates the identification of nearly all the peaks detected by the FID. The concentrations of all the major

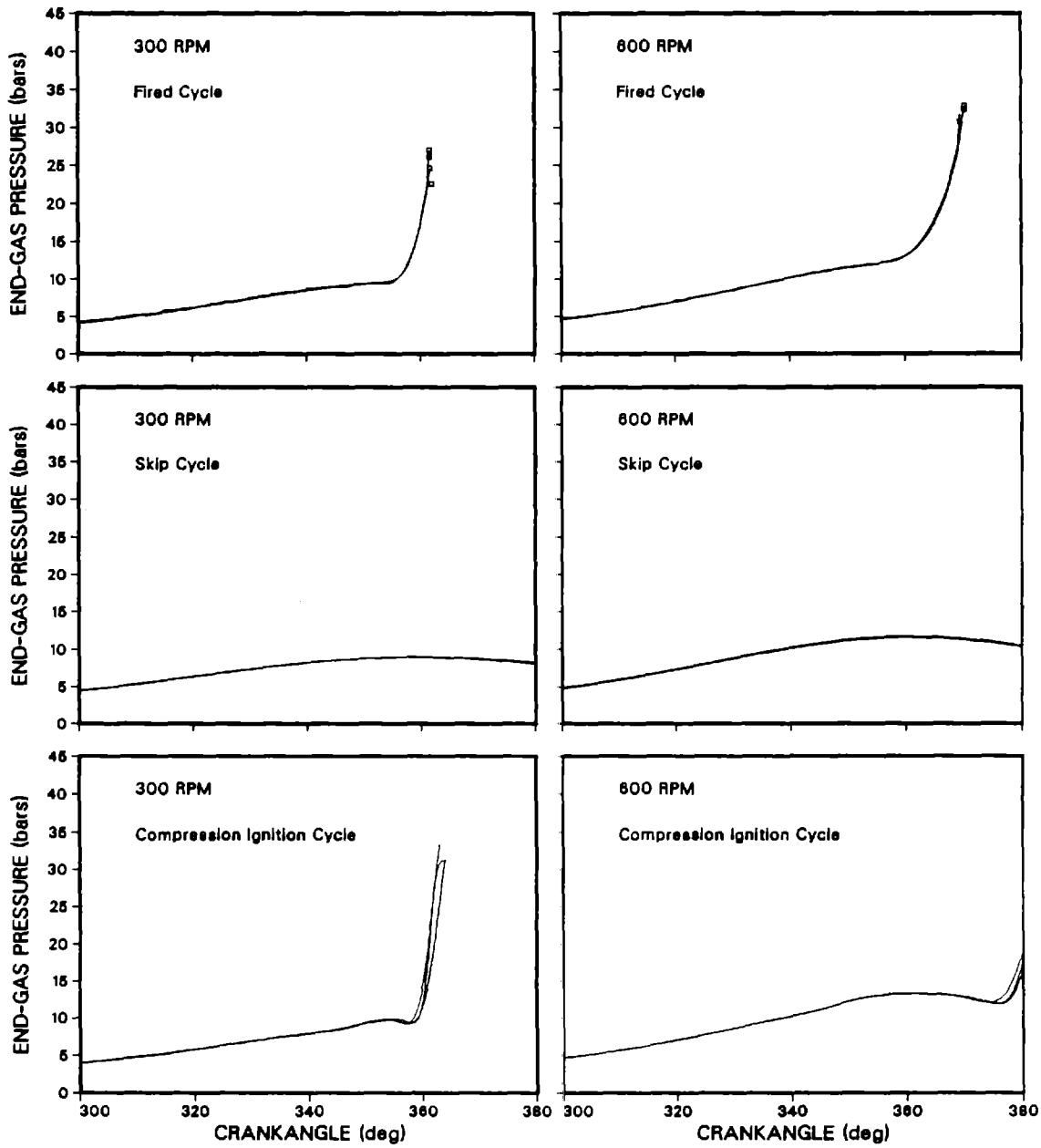

Figure 3. End-gas pressure histories obtained at a resolution of 1 CAD and shown as a function of engine speed. Engine operating conditions: equivalence ratio, 0.85; ignition timing on the firing cycle, 352 CAD; manifold temperature and pressure, 435K and 1.64 bar (300 rpm) and 428K and 1.77 bar (600 rpm).

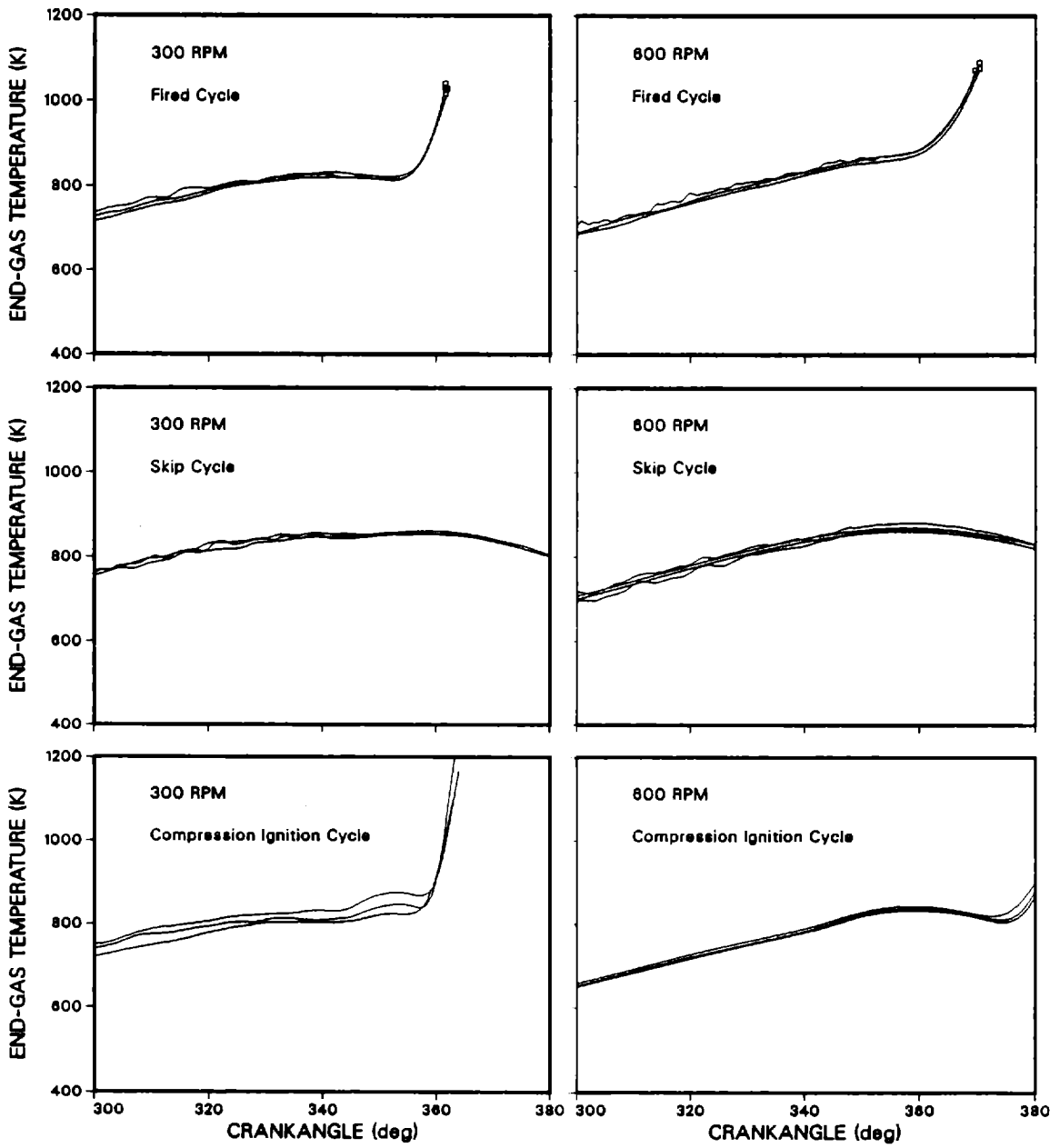

Figure 4. End-gas temperature histories computed from the measured pressure history and shown as a function of engine speed. Engine operating conditions: equivalence ratio, 0.85; ignition timing on the firing cycle, 352 CAD; manifold temperature and pressure, $435K$ and 1.64 bar (300 rpm) and $428K$ and 1.77 bar (600 rpm).

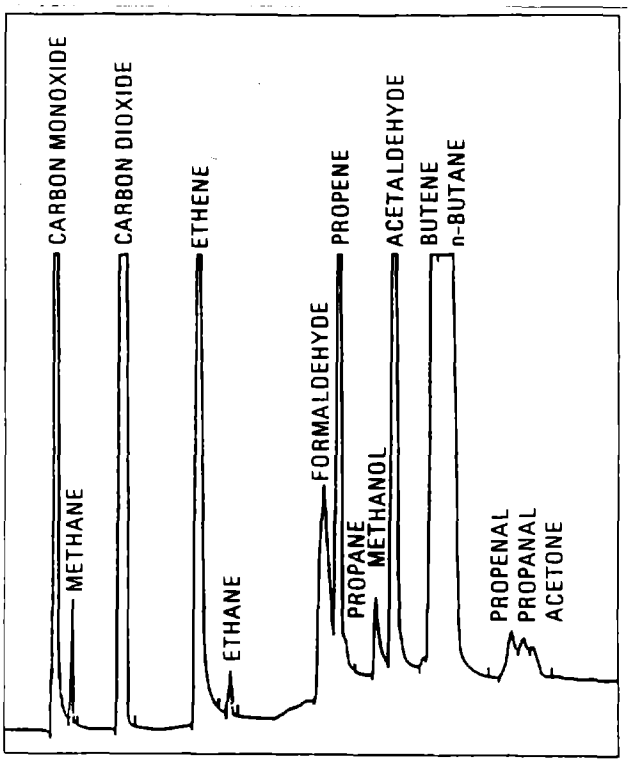

Figure 5. A typical chromatogram illustrating the stable species identified in the analysis of the gas samples.

components of the sample were easily determined. However, for some of the minor components, where there was partial (or even total) overlapping of peaks, it was difficult to estimate the concentrations, since it is the integrated area under the peak that determines the volume fraction of the particular species. An example of this was propane which appeared as a shoulder peak on the dominant species, propene. Since the propane concentration is always small relative to propene, we combined the two when overlapping occurred.

Figure 6 displays species concentration histories as a function of crankangle for the primary aldehyde and alkene intermediates, i.e., formaldehyde, acetaldehyde, ethene, propene and butene. Data are presented for each engine speed and type of engine cycle, and terminate just prior to the autoignition points for the fired and compression ignition cycles and late in the expansion stroke for the skip cycle. At 300 rpm, the dominant species are acetaldehyde and formaldehyde, except for the fired cycle where the ethene concentration jumps ahead just prior to knock. At 600 rpm, the aldehydes are much less prominent, particularly the formaldehyde. This was attributed to the loss of catalyst activity in our analytical system which significantly decreased our sensitivity for formaldehyde and somewhat reduced our sensitivity for acetaldehyde (higher oxygenates were less seriously affected). If we were to correct for this factor, which we cannot quantify at this time, we would expect the aldehydes to show a dominant role at 600 rpm as well.

These data indicate that at the higher engine speed, where there are less losses in the system and therefore slightly higher temperatures, preignition reactions are initiated earlier, but do not proceed as far as the lower speed case where more overall time is available for the end-gas reactions to occur. The fired cycles and the skip cycles, which have very similar initial compositions since they both follow a hot ignition event, show nearly identical reaction histories up to the point of spark ignition and flame propagation in the fired cycles. At that point, the preignition reactions in the fired cycles accelerate due to the rapidly rising pressure and temperature, but are prevented from proceeding too far by the autoignition event.

The compression ignition cycles, on the other hand, show markedly different behavior. They start out with initial intermediate species concentrations that are characteristic of the partially oxidized residual from the prior non-autoigniting skip cycle. Subsequently, the preignition reactions commence earlier in the cycle and proceed much further, eventually leading to an autoignition event.

Similar data for methanol, higher aldehydes and oxygenates, and higher hydrocarbons are shown in Fig. 7. These data have the same behavior and characteristics as the alkenes and lower aldehydes. Comparable CO and CO_2 data are unavailable due to the catalyst activity problem discussed above.

NUMERICAL MODEL AND CHEMICAL KINETIC MECHANISM

We performed the computer modeling analysis using the HCT program [30], which solves the coupled chemical kinetics and energy equations. The detailed chemical kinetic reaction mechanism was based on a series of previous studies in which we examined the oxidation of fuels as large as n-butane, isobutane, and n-pentane [1,21,31,32,33,34]. Reverse reaction rates are computed from the forward rates and the appropriate thermodynamic data [35,36]. In cases where thermochemical data were not available, reverse reaction rates were estimated. This mechanism has been shown to describe the high temperature (greater than $1000K$) oxidation of many hydrocarbon fuels, including hydrogen, carbon monoxide, methane, methanol, acetylene, ethylene, ethane, propane, propene, n-butane, isobutane, and n-pentane in a wide variety of combustion environments. For some reactions, we included pressure dependences from Miller and coworkers [37] and Tsang and Hampson [38]. For reactions whose pressure dependence was not available, we assumed either a high or low pressure limit for the reaction rate.

During the engine cycle, the end gas is subjected to temperatures in the range of $450K$ to $800K$ for a considerable length of time (as long as 70 ms at the slower

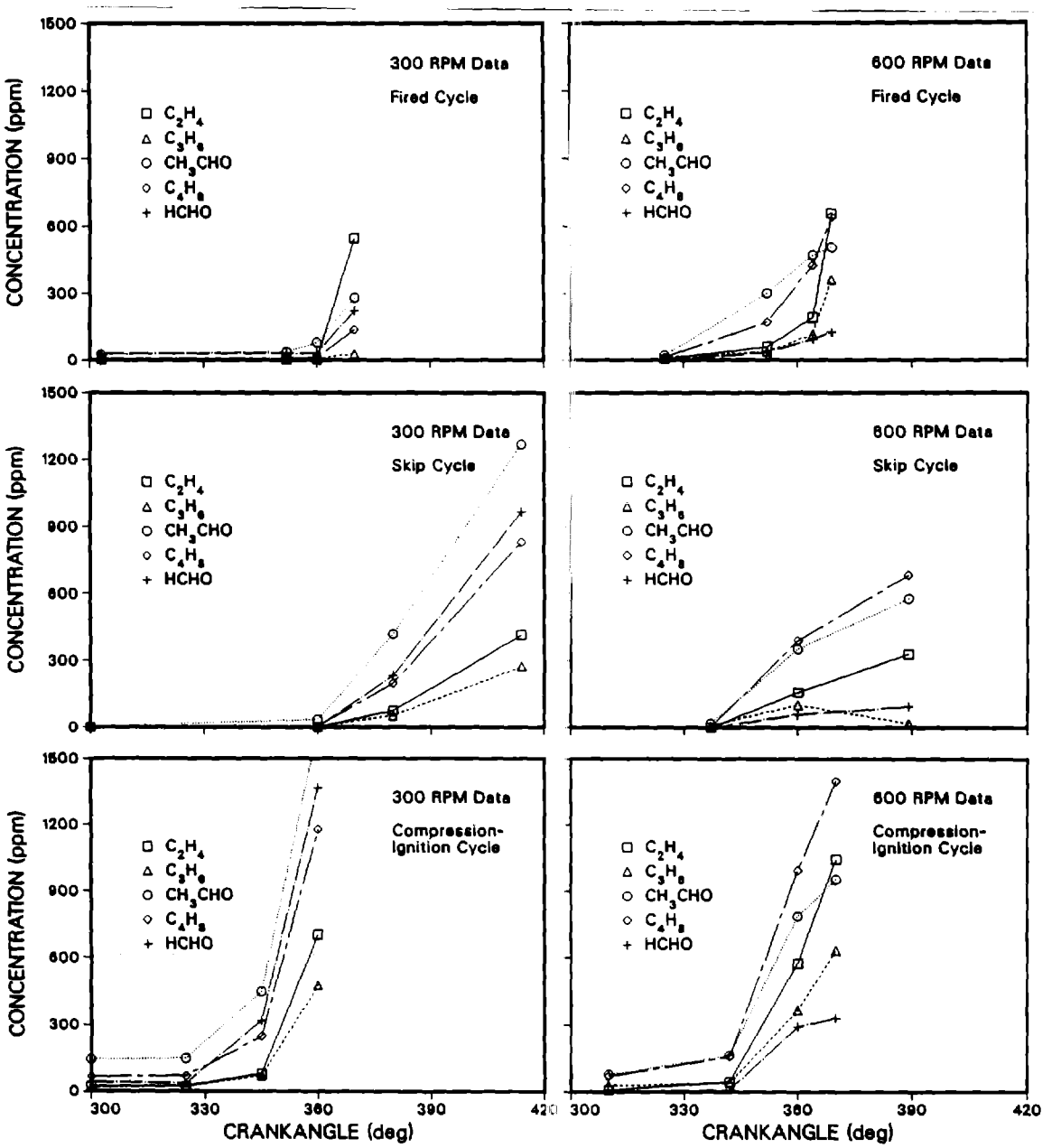

Figure 6. Concentration histories of the principal olefins and aldehyde species illustrated for the time interval around TDC. The data is illustrated as a function of engine speed for the firing cycle, the skip cycle and the compression ignition cycle.

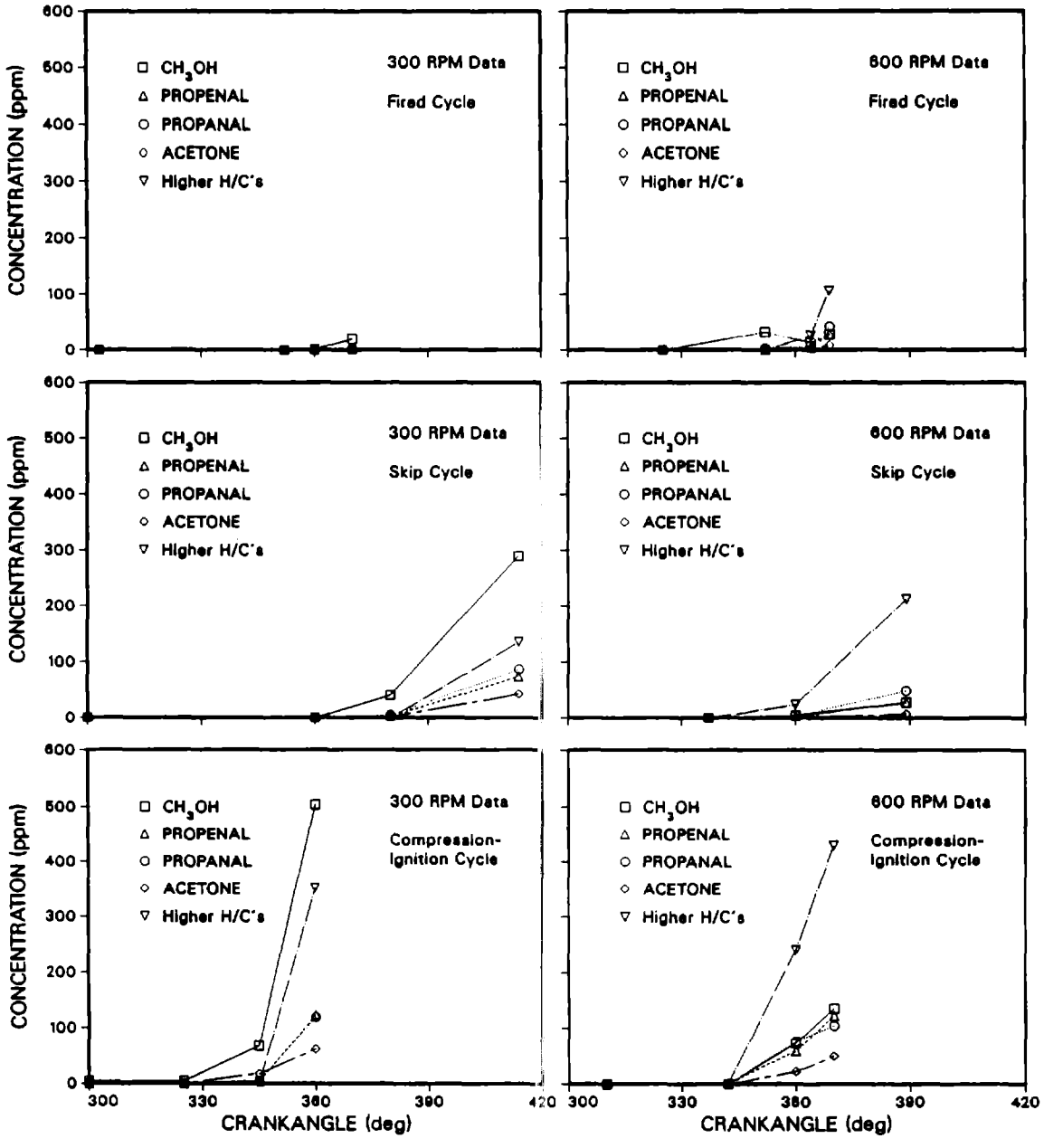

Figure 7. Concentration histories of the other important oxygenated species illustrated for the time interval around TDC. The data is illustrated as a function of engine speed for the firing cycle, the skip cycle and the compression ignition cycle.

engine speeds considered in the present work). Reaction pathways that are unimportant at temperatures above $1000K$ may have sufficient time during the engine cycle to influence the overall rate of autoignition. As a result, chemical kinetic descriptions of these pathways must be included in the overall reaction mechanism. These reactions involve primarily the addition of molecular oxygen to the important alkyl radicals and their subsequent production of hydroperoxides that then decompose and provide chain branching. Many of these additional reactions are tabulated and discussed in previous modeling studies of low temperature hydrocarbon oxidation [32,33,39,40,41]. For the present study, we have extended the low temperature portions of the reaction mechanism to include the p-butyl, s-butyl and other radicals that are important in the oxidation of n-butane. Where possible, the reactions and their rate expressions have been based on kinetic studies from the combustion literature. We estimated rates of the addition of molecular oxygen to alkyl radicals from the work of Slagle and Gutman [42,43]. Particularly valuable was the work of Baker et al. [40,41], in which small amounts of n-butane were added to slowly reacting mixtures of hydrogen and oxygen at $753K$ in a static reactor. They described the internal H-atom abstractions of the n-butyl peroxy radical and provided estimates of the associated rate constants based on their measurements of species concentrations. We have employed their estimates of the rates of the internal H-atom abstractions of the n-butylperoxy radical. These reactions lead to additional radical production at low temperatures and accelerate the overall oxidation rate of n-butane.

MODELING PROCEDURE - We numerically simulated the sequence of engine cycles that were experimentally investigated at 300 and 600 rpm. The model assumes that the only way in which the end gas interacts with the remainder of the combustion chamber is through the compressional work done on the end gas by the moving piston and, when spark ignition occurs, by the flame front. Transport processes in the end gas are neglected.

The initial composition of the end gas consists of n-butane and air, combined with the residual gas from the previous cycle. In the cases of the fired and the skip cycles, the residual gas consists entirely of N_2, CO_2, and H_2O. This residual gas composition is a result of the prior cycle in which the fuel-air mixture was fully oxidized. In the case of the compression ignition cycle, the residual gas is composed of reactants that underwent partial oxidation in the previous cycle.

Throughout the computations, the measured end-gas pressure history is followed. However, the end-gas temperature history, determined using the thermodynamic analysis, is imposed only until the calculation indicates that heat release due to chemical reaction in the end gas has become significant. The end-gas temperature is then computed directly by the kinetics model, thus including the effects of heat release in the end gas. The advantage of this approach is that it allows us to include as much engine operating data as possible in the model. Processes such as flame propagation in the other parts of the engine chamber, piston motion, and heat transfer to the engine walls are incorporated. On the other hand, if significant heat release occurs due to reactions not included in the kinetic model, then this heat release is unaccounted for in the numerical simulation. The computed results discussed below indicate that the kinetic model reproduces most of the measured species concentrations and suggests that we have included most of the important reaction paths.

MODELING RESULTS - Table 1 compares the computed and measured times of autoignition for fired cycles. The agreement is within 0.3 ms for each case, indicating the model can accurately predict the effects of engine speed on autoignition time.

Table 1

Predicted and Measured Autoignition Times

rpm	Autoignition Time (ms)*	
	Measured	Predicted
300	1.3	1.1
600	2.8	2.5

*Referenced to TDC of the compression stroke

In Tables 2 and 3, we compare measured species concentrations with modeling predictions for the skip cycle. The measured concentrations listed are at the last measurement time given in Figs. 6 and 7. The calculated species concentrations correspond to a time when the total level of intermediate concentrations are about the same as observed in the experiment. We have chosen this method of comparison since the rate of production of intermediates was faster in the calculation for the 300 rpm case (see below), and we want to evaluate how well the model predicts relative rankings of intermediates.

There is mixed agreement between the model predictions and the experimental observations for the major intermediates. For the two intermediates measured in the highest concentration, C_4H_8 and CH_3CHO, the agreement is good for the 600 rpm case (Table 3); however, at 300 rpm, the model predicts too little CH_3CHO relative to C_4H_8 (Table 2). The agreement for the smaller olefins, C_3H_6 and C_2H_4, is excellent at 300 rpm, and at 600 rpm, the comparison for C_2H_4 is satisfactory, but the measured concentration for C_3H_6 is likely an anomalous data point. The calculated concentration probably indicates the appropriate level and is consistent with the trend in the other measured species concentrations in Fig. 6.

Table 2

Species Concentrations Near the End of the Skip Cycle (300 rpm)

Species	Measured Conc.(ppm)	Predicted Conc.(ppm)
C_4H_8	820	957
CH_3CHO	1260	730
C_2H_4	400	400
C_3H_6	270	255
CH_2O	920	1150
CH_3OH	292	70
propanal	87	15
propenal	74	8
acetone	45	-
C_4H_{10}	16800	18700
C_4H_{10} (initial)	-	21400
time [ms]	39.0	-3.0
Temperature [K]	-	860

Table 3

Species Concentrations Near the End of the Skip Cycle (600 rpm)

Species	Measured Conc.(ppm)	Predicted Conc.(ppm)
C_4H_8	700	720
CH_3CHO	550	480
C_2H_4	350	266
C_3H_6	10	192
CH_2O	100	750
CH_3OH	133	44
propanal	105	8
propenal	119	5
acetone	52	-
C_4H_{10}	16800	17700
$C_4H_{10}(initial)$	-	21400
time [ms]	8.3	5.0
Temperature [K]	790	847

The predicted levels of secondary intermediates (CH_3OH, propanal, and propenal) are lower than those measured. These species evolve at later times in the calculation with the levels of these intermediates eventually growing to approximately the same levels observed experimentally. Finally, the model predicted negligible concentrations of acetone.

It is interesting to compare the predicted extent of reaction in the skip cycle with that observed experimentally. We use the level of intermediates as a convenient indicator of the extent of reaction, and compare the level of intermediates predicted with those measured at the time of the last species measurement in the skip cycle. At 600 rpm, the predicted extent of reaction is only about 10 percent larger than the measured value. At 300 rpm, the calculated extent of reaction is about twice that measured.

Although the kinetic model gave reasonable results for the knocking and skip cycles at both engine speeds, it did not predict autoignition for the compression ignition cycle. If the reaction rate constants of a few key reaction are increased, the model does predict autoignition for this cycle. Specifically, these rate constants are for internal H-atom abstractions of the butylperoxy radical (discussed in the next section). The value of these rate constants is not known to better than a factor of two, and we increased them by 50 percent. Autoignition in the compression ignition cycle was then computated at 600 rpm. The predicted autoignition time is 6.3 ms compared to the experimental value of 5 ms. However, with the increased rate constants, the model predicts autoignition during the skip cycle at 300 rpm. Consequently, we were unable to develop a model which exhibited the experimentally observed behavior under every condition.

We used the model to determine the temperature at the experimentally observed time of autoigntion. This temperature was evaluated at the time in the calculation when the computed levels of intermediate species reached the levels of those observed experimentally, just prior to autoignition. The level of intermediates at this time is illustrated in Figs. 6 and 7 for the fired and compression ignition cycles. We used the calculated results at 600 rpm (the condition where the model correctly indicates autoignition in the fired and compression ignition cycles). In both cycles, the temperature just before autoignition was approximately $910 \pm 10K$. Thus, despite the large differences in extent of reaction as indicated by the measured levels of intermediates just before autoignition (Figs. 6 and 7), the calculations indicate approximately the same temperature at the observed time of autoignition. Also, the calculated radical levels, as evidenced by the key OH radical, are about the same ($2 - 5 \times 10^{-8}$ mole fraction) just prior to autoignition for both cycles. This constancy in the temperature at the time of autoignition is in agreement with the experimental measurements of Gluckstein and Walcutt [9]. They found the temperature at the time of autoignition to be $1022 \pm 22K$ for most mixtures of primary reference fuels that they investigated.

DISCUSSION OF CHEMICAL KINETICS - The chemical reaction paths that are important at the high pressures and intermediate temperatures encountered in present study are different from those that are important at the more frequently studied conditions of high temperature and atmospheric pressure. At one atmosphere and approximately $1000K$, hydrocarbon oxidation is controlled by the production of H atoms and chain branching via [24],

$$H + O_2 = O + OH$$

At the higher pressures and lower temperatures addressed in the present study, the rate of oxidation is controlled by the production of peroxy radicals including HO_2 and by chain branching through the mechanisms discussed below.

When the fuel consumption begins at temperatures of approximately $820K$, the reactions responsible for OH production are mainly of two types. The first type involves isomerizations of butylperoxy radicals. These isomerization reactions lead to the production of acetaldehyde, formaldehyde, other oxygenates, and OH radicals. For example, the main isomerization route for the p-butylperoxy radical is

$$\begin{aligned}
&CH_3CH_2CH_2CH_2 + O_2 = CH_3CH_2CH_2CH_2O_2\\
&CH_3CH_2CH_2CH_2O_2 = CH_3CHCH_2CH_2O_2H\\
&CH_3CHCH_2CH_2O_2H + O_2 =\\
&\qquad CH_3CH(O_2)CH_2CH_2O_2H\\
&CH_3CH(O_2)CH_2CH_2O_2H =\\
&\qquad CH_3CHO + CH_2O + CH_2O + OH \qquad (1)
\end{aligned}$$

where the products in Reaction 1 were suggested by Baker et al. [41]. An analogous isomerization path occurs for the s-butylperoxy radical, and both paths were included for this study. It is important to note that this reaction sequence produces the reactive OH radical, and a significant amount of heat release occurs since the reaction sequence is exothermic by approximately 102 kcal/mole. Additional heat release is obtained when the OH radical reacts with the fuel,

$$C_4H_{10} + OH = C_4H_9 + H_2O \qquad (2)$$

and forms water (C_4H_9 refers to either p-butyl and s-butyl, which were considered separately in this study). This reaction is exothermic by approximately 23 kcal/mole and is one of the most important sources of heat release in the oxidation of n-butane.

The other type of reactions that produce OH during the early stages of fuel oxidation are:

$$\begin{aligned}
CH_3 + O_2 + M &= CH_3O_2 + M\\
C_4H_{10} + CH_3O_2 &= C_4H_9 + CH_3O_2H\\
CH_3O_2H &= CH_3O + OH
\end{aligned}$$

where M represents an arbitrary third body.

This reaction sequence is chain branching since one CH_3 radical is consumed and two radicals, CH_3O and OH, are produced. The reaction sequence produces a significant amount of OH radicals and significantly accelerates the oxidation rate of the fuel. Again, the OH radicals formed react with the fuel (Reaction 2) and release a significant amount of heat.

When the temperature of the n-butane-air mixture reaches about $950K$, a temperature achieved only during cycles with spark or compression ignition, radical production occurs primarily through reactions involving HO_2:

$$\begin{aligned}
C_4H_{10} + HO_2 &= C_4H_9 + H_2O\\
H_2O_2 + M &= OH + OH + M
\end{aligned}$$

This reaction path is also chain branching and greatly accelerates the autoignition process. It is the main path for OH production during a large part of the oxidation of n-butane under the present conditions. The OH radicals formed then react with the fuel (Reaction 2), contributing to heat release.

It is interesting to compare the reactions that are important in the autoignition of n-butane with those that are important in autoignition of isobutane. This comparison is of interest since isobutane is a branched isomer of n-butane and is much more resistant to knock that n-butane. In general, branched alkanes have higher critical compression ratios and are more resistant to knock than straight-chain alkanes [44].

Table 4 gives the reaction sensitivities for n-butane and isobutane. The reaction sensitivities for isobutane were obtained in a previous study [1]. These quantities were calculated by multiplying the forward and reverse reaction rate by a factor of two and observing the change in the autoignition time. The sensitivities in Table 4 were calculated from

$$\text{percent sensitivity} = 100(\tau' - \tau)/\tau_f$$

where τ is the baseline autoignition time, and τ' is the autoignition time with the rate of the given reaction multiplied by a factor of two. We normalized the difference between τ' and τ by the characteristic fuel consumption time τ_f for the baseline case. τ_f is the interval between the time the fuel concentration decreases by one percent of its inital value and the time of autoignition.

The autoignition time for n-butane is most sensitive to the rate of isomerization of butyl-peroxy radicals (Reaction vi). The autoignition time for isobutane is most sensitive to the rate of reaction between HO_2 and the fuel (Reaction i). The isomerization of peroxy radicals is a reaction path that is characteristic of chemistry that occurs at low temperatures, while reactions involving HO_2 are characteristic of chemistry that is important at higher temperatures. This observation suggests that low temperature chemistry is more important

Table 4

Reaction Rate Sensitivity
(Based on autoignition time)

	Reaction			Sensitivity N-Butane	Sensitivity Isobutane
i.	$C_4H_{10} + HO_2$	=	$C_4H_9 + H_2O_2$	-11.4	-13.1
ii.	$C_4H_{10} + CH_3O_2$	=	$C_4H_9 + CH_3O_2H$	-4.4	-7.6
iii.	$HO_2 + HO_2$	=	$H_2O_2 + O_2$	1.7	-7.3
iv.	$H_2O_2 + M$	=	$OH + OH + M$	-9.2	-7.1
v.	$CH_3 + HO_2$	=	$CH_3O + OH$	-2.3	-6.1
vi.	$C_4H_9O_2$	=	$C_4H_8O_2H$	-39.5	-4.5
vii.	$C_4H_9 + O_2$	=	$C_4H_8 + HO_2$	4.3	4.0
	Temperature at which $[C_4H_{10}] = 0.99[C_4H_{10}]_{initial}$			$820K$	$975K$

in the autoignition of n-butane than in the autoignition of isobutane. This trend is further substantiated by the last entry in Table 4 which is the temperature at which significant fuel consumption starts to occur in the calculation. Significant fuel consumption begins at a temperature that is about $55K$ lower for n-butane than for isobutane.

There are significant differences in the chemical kinetic behavior of the fuel-air mixtures in the skip cycle and in the compression ignition cycle. These differences are due to the compositions of the residual gases in each cycle. In the skip cycle, the residual fraction consists of N_2, O_2, CO_2, and H_2O while in compression ignition cycle, the residual fraction consists of partially reacted fuel and air. We performed a series of calculations to assess the effect of the composition of the residual gas on extent of reaction during the skip cycle and the compression ignition cycle. We used the same experimental pressure and temperature history for all these calculations. The first calculation was for the case where the residual gas was entirely burnt products, representative of the skip cycle. The initial radical production during the skip cycle occurs by the relatively slow reaction

$$C_4H_{10} + O_2 = C_4H_9 + HO_2 \qquad (3)$$

which produces the HO_2 radical. This leads to a slow initial development of the radical pool. The accelerating processes discussed earlier become dominant only when Reaction 3 has increased the initial radical concentrations sufficiently. We calculate that only 10 percent of the initial fuel is consumed during this cycle (Table 5).

We also examined the case where the residual fraction was partially reacted fuel-air mixture. This calculation is representative of chemistry occurring in the compression ignition cycle. The partially reacted fuel-air residual was obtained from the final mixture concentrations calculated from the skip cycle. In this calculation, 36 percent of the fuel is consumed during the engine cycle (Table 5). There are probably some key reactive species in the residual fraction that lead to the further extent of reaction when the residual is partially reacted fuel. In order to determine the identity of these reactive species, we selectively removed certain species from the residual fraction.

Table 5

Effect of Residual Composition on Overall Extent of Reaction

Residual Composition	Fraction of Initial Fuel Consumed
partially reacted fuel-air	36%
partially reacted with aldehydes & olefins = 0	36%
partially reacted with RO_2 = 0	23%
partially reacted with all radicals = 0	19%
partially reacted with peroxides = 0	14%
burnt products (N_2, O_2, CO_2, H_2O)	10%
unreacted fuel-air	20%

The results presented Table 5 show that the removal of peroxides from the partially reacted residual gas had the largest effect on the extent of reaction, while removal of the aldehydes and olefins had no significant effect. The peroxides increase the reactivity of the initial mixture since they fall apart during the early part of the cycle and give two radicals:

$$RO_2H = RO + OH$$

This radical production accelerates the growth of the initial radical pool. The growth of the radical pool in this case is not limited by the slow process of Reaction 3 as in the previous case when the residual was burnt products. This faster initial growth of the radical pool leads to an increase in the overall oxidation rate during the compression ignition cycle.

Another difference between the skip and compression ignition cycles that leads to a faster oxidation rate in the latter, is that the concentrations of fuel, intermediates and molecular oxygen are higher in the compression ignition cycle. The fuel-air mixture in the skip cycle is diluted by a residual fraction consisting of N_2, CO_2 and H_2O, but the compression ignition cycle has fuel and partially oxidized intermediates in its residual fraction. Higher concentrations of fuel and intermediates lead to higher alkyl radical concentrations. The rates of reaction paths discussed above that generate OH radicals during fuel oxidation all depend on the product of the concentration of alkyl radicals and O_2, both of which are higher in the compression ignition cycle. For example, for the n-butylperoxy isomerizations (reaction path (1) above), the overall rate is dependent on the product $[C_4H_9][O_2]$. The rate of chain branching from methyl hydroperoxide is dependent on the product $[CH_3][O_2]$. Both of these accelerating paths are more rapid as a consequence of the higher concentrations of alkyl radicals and molecular oxygen found in the compression ignition cycle.

We examined the effect of the initial mixture in the skip cycle being more diluted than the initial mixture of the compression ignition cycle. We compared the calculation where the fuel-air mixture is diluted by burnt products to a calculation where the entire initial mixture is unreacted fuel-air mixture. The extent of reaction increases from 10 to 20 percent when the residual is changed from burnt products to unreacted fuel-air mixture (Table 5). Note that the extent of reaction with a residual of partially reacted fuel-air is 36 percent. Thus, the greater extent of reaction in the compression ignition cycle compared to the skip cycle is only partially explained by higher concentrations of fuel, intermediates and O_2 in the initial mixture. The complete explanation must include the effect of reactive species, particularly peroxides, in the partially reacted fuel-air residual.

DISCUSSION

These experimental observations and kinetic modeling simulations of the compression ignition behavior of a spark ignition engine fueled with n-butane confirm some of our previous speculations about the chemical aspects of end-gas autoignition and provide us with some interesting new insights into the controlling phenomena. The most striking characteristic of the compression ignition process is that under the operating conditions that we observed, compression ignition occurs only on a skip cycle that follows another skip cycle. While this certainly was the case for the data reported above, we found it also to be true when we operated under conditions where we skipped three, four or even five cycles between fired cycles. This seems to indicate that the residual products of hot combustion or recycled intermediates resulting from partial oxidation of the fuel carried over from the previous cycle and mixed with the fresh incoming fuel-air charge have important effects on the chemistry preceding the autoignition.

There are a number of plausible arguments that can explain this observed effect of the recycled residuals. First, the approximately 20% fraction of residuals mixed with the fresh charge will lead to a strong diluting of the fuel-air mixture undergoing compression and heat release. As a result, preflame chemical activity will not be as effective in increasing the end-gas temperature. On the other hand, it is possible that the presence of both carbon dioxide and water vapor may result in some kinetic impediment to the preflame reactions, reducing the heat released by the low temperature chemical activity. The ultimate outcome of either scenario is the same as described above; that is, the increase in the end-gas temperature due to preflame chemistry will be less significant. Finally, since we observed that as much as 10 to 20% of the fuel is consumed during the compressional heating of the skip cycle, it is possible that the presence of these products of partial oxidation may enhance the low temperature end-gas chemistry, perhaps through a mechanism of early formation of radical species. Our calculations indicate that the peroxide species are a primary link to the formation of these radicals.

The importance of the preflame reactions is evident when it is observed that without preflame chemistry, the end-gas temperature on a cycle following a skip cycle will be lower than the temperature on a cycle following a hot combustion event. Clearly, the residuals from a skip cycle will be much cooler than those from a fired cycle. Furthermore, the engine surfaces are likely to be somewhat cooler following a skip cycle. A careful examination of the data presented in Figures 2 and 3 supports this argument in that the pressures and computed temperatures on the compression ignition cycle do appear to be a little lower than those for the firing

and skip cycles. Thus, the fact that the compression ignition occurs on a cycle where the initial end-gas temperature is lower, provides very strong support to the importance of the low temperature chemistry in supplying heat to increase the end-gas temperature to a level consistent with autoignition.

In many previous investigations of the autoignition behavior of different hydrocarbon fuels, it has been proposed that the role of preflame chemistry in the autoignition process is primarily to provide heat release to raise the end-gas temperature to a level where the reactions of hot ignition will proceed. The end-gas sampling measurements reported in the present work provide strong evidence supporting this contention. If we compare the intermediate species concentrations measured just before autoignition on the fired cycle with those of the compression ignition cycle, we see a significant difference in the concentration levels. Indeed, for the case of the 300 rpm data, the concentrations are a factor of 3 to 4 less on the firing cycle; while in the case of the 600 rpm data the concentrations are about a factor of two less on the firing cycle (the engine speed effect being due to the amount of time available for reaction). This large disparity in the intermediate concentration levels just prior to autoignition leads us to speculate that the chemical extent (and perhaps even the nature) of the preflame reactions is important to the autoignition process only insofar as it affects the end-gas temperature.

Certain other characteristics of the present data also provide credibility for the hypothesis regarding the role of the preflame reactions. The pressure record for the compression ignition cycle illustrated in Figure 2(a) clearly shows that the heat released prior to autoignition is sufficient to cause a measurable increase in the pressure. Thus, in any analysis of the chemistry preceding autoignition, the temperature increase due to this heat release must be considered in order to specify properly the thermodynamic conditions. This clearly illustrates the need to model the preflame heat release correctly using the kinetic model and to verify the predictions by actually measuring the end-gas temperature history.

SUMMARY

The results of this study have provided some exciting new insight into our study of autoignition and knock in spark ignition engines through observations of the process of compression ignition. This work has strengthened the hypothesis that the role of the low temperature end-gas chemistry is to provide enough heat release that the end-gas temperature increases to a level where hot ignition can occur. Furthermore, this work has pointed out that the recycled residual products of combustion have a significant influence on the end-gas reactions. We are not yet sure how this effect perturbs the chemistry, and we are continuing our studies in order to address this issue.

ACKNOWLEDGMENT

This work was performed at the Combustion Research Facility at Sandia National Laboratories and at the Lawrence Livermore National Laboratory (under contract number W-7405-ENG-48) and was supported by the U.S. Department of Energy, Division of Energy Conversion and Utilization Technologies. We are grateful to Professor Colin Ferguson of Purdue University for his efforts in developing a comprehensive, thermodynamic heat-release analysis for processing our experimental pressure data. We wish to thank Professors David Foster and James Keck and Dr. James Miller for their careful review of the manuscript of this paper and their helpful suggestions. We especially wish to thank Professor Fred Dryer for his assistance and effort in setting up the gas sampling and analytical species analysis equipment and for the many stimulating discussions and suggestions regarding the results of this study.

REFERENCES

1. Green, R.M., Parker, C.D., Pitz, W.J. and Westbrook, C.K., "The Autoignition of Isobutane in a Knocking Engine," SAE Paper No. 870169 (1987).

2. Smith, J.R., Green, R.M., Westbrook, C.K. and Pitz, W.J., "Experimental and Modeling Study of Engine Knock," Twentieth Symposium (International) on Combustion/The Combustion Institute, p 91 (1984).

3. Egerton, A., Smith, F.Ll. and Ubbelohde, A.R., "Estimation of the Combustion Products from the Cylinder of the Petrol Engine and its Relation to 'Knock'," Phil. Trans. of the Royal Society of London, Ser A, n 744, v 234, p 433 (1935).

4. Downs, D., Walsh, A.D. and Wheeler, R.W., "A Study of the Reactions that Lead to 'Knock' in the Spark Ignition Engine," Phil. Trans. of the Royal Society of London, Ser A, v 243, p 462 (1951).

5. Downs, D., Griffiths, S.T. and Wheeler, R.W., "Pre-Flame Reactions in the Spark Ignition Engine: The Influence of Tetraethyl Lead and Other Antiknocks," Jour. of the Inst. of Petrol., v 49, n 469, p 8 (1963).

6. Pahnke, A.J., Cohen, P.M. and Sturges, B.M., "Preflame Oxidation of Hydrocarbons in a Motored Engine," Ind. and Engin. Chem., v 46, n 5, p 1024 (1954).

7. Walcutt, C., Mason, J.M. and Rifkin, E.B., "Effect of Preflame Oxidation Reactions on Engine Knock," Ind. and Engin. Chem., v 46, n 5, p 1029 (1954).

8. Sturgis, B.M., "Some Concepts of Knock and Antiknock Action," SAE Transactions, v 63, p 253 (1955).

9. Gluckstein, M.E. and Walcutt, C., "End-Gas Temperature-Pressure Histories and Their Relation to Knock," SAE Transactions, v 69, p 529 (1961).

10. Johnson, J.H., Myers, P.S. and Uyehara, O.A., "End-Gas Temperatures, Pressures, Reaction Rates, and Knock," SAE Transactions, v 74, p 748 (1965).

11. Halstead, M.P., Kirsh, L.J. and Quinn, C.P., "The Autoignition of Hydrocarbon Fuels at High Temperatures and Pressures - Fitting of a Mathematical Model," Combust. Flame, v 30, p 45 (1977).

12. Najt, P. M., and Foster, D. E., "Compression Ignited Homogeneous Charge Combustion," SAE Paper No. 830264 (1983).

13. Griffiths, J. F., and Nimmo, W., "Spontaneous Ignition and Engine Knock Under Rapid Compression," Combust. Flame, v 60, p 215 (1985).

14. Franck, J., Griffiths, J. F. and Nimmo, W., "The Control of Spontaneous Ignition Under Rapid Compression," Twentyfirst Symposium (International) on Combustion/The Combustion Institute (1986).

15. Wilk, R.D., Cernansky, N.P. and Cohen, R.S., "The Transition in the Oxidation Chemistry of n-Butane from Low to Intermediate Temperatures," Western States Section, The Combustion Institute, Paper No. 85-31 (1985).

16. Wilk, R.D., Cernansky, N.P. and Cohen, R.S., "The Oxidation of Propane at Low and Transition Temperatures," Comb. Sci. and Tech., v 49, p 41 (1986).

17. Lignola, P. G., Piro, R. and Reverchon, E., "Physico-Chemical Investigation on Self-Ignition with Reference to Knocking," Proc. V Task Leaders Conference, IEA (1983).

18. Lignola, P. G. and Reverchon, E., "Cool Flames," Prog. Energy Comb. Sci., v 13, p 75 (1987).

19. Natarajan, B. and Bracco, F.V., "On Modeling Auto-Ignition in Spark-Ignition Engines," Combust. Flame, v 57, p 179 (1984).

20. Keck, J.C., and Hu, Haoran, "Explosions of Adiabatically Compressed Gases in a Constant Volume Bomb," the Twentyfirst Symposium (International) on Combustion/The Combustion Institute (1986).

21. Pitz, W.J. and Westbrook, C.K., "Chemical Kinetics of the High Pressure Oxidation of n-Butane and Its Relation to Engine Knock," Combust. Flame, n 63, p 113 (1986).

22. Cernansky, N.P., Green, R.M., Pitz, W.J. and Westbrook, C.K., "Chemistry of Fuel Oxidation Preceding End-Gas Autoignition," Comb. Sci. and Tech., v 50, n 1-3, p 3 (1986).

23. Leppard, W.R., "A Detailed Chemical Kinetics Simulation of Engine Knock," Comb. Sci. and Tech., v 43, p 1 (1985).

24. Westbrook, C.K. and Dryer, F.L., "Chemical Kinetic Modeling of Hydrocarbon Combustion," Prog. Energy Combust. Sci. n 10, p 1 (1984).

25. Johnston, S.C., Robinson, C.W., Rorke, W.S., Smith, J.R. and Witze, P.O., "Application of Laser Diagnostics to an Injected Engine," SAE Trans., n 88, p 353 (1979).

26. Ferguson, C.R., Green, R.M. and Lucht, R.P., "Unburned Gas Temperatures in an Internal Combustion Engine: II. Heat Release Computations," Accepted for publication in Comb. Sci. and Tech. (1986).

27. Green, R.M. and Lucht, R.P., "An Application of Laser Diagnostics to the Study of End-Gas Autoignition and Engine Knock," Trans. of COMMODIA - International Symposium on Diagnostics and Modeling of Combustion in Reciprocating Engines, Tokyo, Japan, p 259 (1985).

28. Lucht, R.P., Green, R.M., Palmer, R.E, Teets, R.E. and Ferguson, C.R., "Unburned Gas Temperatures in an Internal Combustion Engine: I. CARS Temperature Measurements," Accepted for publication in Comb. Sci. and Tech. (1986).

29. Taylor, C.F., Taylor, E.S., Livengood, J.C., Russell, W.A. and Leary, W.A., "Ignition of Fuels by Rapid Compression," SAE Quart. Trans., v 4, n 2, p 232 (1950).

30. Lund, C.M., "HCT - a General Computer Program for Calculating Time-dependent Phenomena Involving One-dimensional Hydrodynamics, Transport, and Detailed Chemical Kinetics," Lawrence Livermore National Laboratory, Report No. UCRL-52504 (1978).

31. Pitz, W.J., Westbrook, C.K., Proscia, W.M. and Dryer, F.L., "A Comprehensive Chemical Kinetic Reaction Mechanism for the Oxidation of n-Butane," Twentieth Symposium (International) on Combustion/The Combustion Institute, p 831 (1984).

32. Kaiser, E.W., Westbrook, C.K. and Pitz, W.J., "Acetaldehyde Oxidation in the Negative Temperature Coefficient Regime: Experimental and Modeling Results," Int. J. Chem. Kinet., v 18, p 655 (1986).

33. Wilk, R.D., Cernansky, N.P., Pitz, W.J. and Westbrook, C.K., "Chemical Kinetic Modeling of Propene Oxidation at Low and Intermediate Temperatures," Western States Section, The Combustion Institute, Paper No. 87-42 (1987).

34. Westbrook, C.K., Pitz, W.J., Thorton, M.M. and Malte, P.C., "A Kinetic Modeling Study of n-Pentane Oxidation in a Jet-Stirred Reactior," Western States Section, The Combustion Institute, Paper No. 87-41 (1987).

35. JANAF Thermochemical Tables, U.S. Government Printing Office, Washington, D.C. (1971).

36. Benson, S.W., Thermochemical Kinetics, Wiley, New York (1976).

37. Glarborg, P., Miller, J.A. and Kee, R.J., "Kinetic Modeling and Sensitivity Analysis of Nitrogen Oxide Formation in Well-Stirred Reactors," Combust. Flame, v 65, p 177 (1986).

38. Tsang, W. and Hampson, R.F., "Chemical Kinetic Data Base for Combustion Chemistry. Part 1. Methane and Related Compounds," Jour. Phys. Chem. Ref. Data, v 15, p 1087 (1986).

39. Wilk, R.D., Cohen, R.S. and Cernansky, N.P., "An Experimental Study of Propene Oxidation at Low and Intermediate Temperatures," Comb. Sci. and Tech., v 52, p 39 (1986).

40. Baker, R.R., Baldwin, R.R., Fuller, A.R. and Walker, R.W., "Addition of $n - C_4H_{10}$ and C_4H_8 to Slowly Reacting Mixtures of Hydrogen and Oxygen at $480C$. Part 1. - Formation of Hydrocarbon Products," J. Chem. Soc., Faraday Trans. I, v 71, p 736 (1975).

41. Baker, R.R., Baldwin, R.R. and Walker, R.W., "Addition of $n - C_4H_{10}$ and C_4H_8 to Slowly Reacting Mixtures of Hydrogen and Oxygen at $480C$. Part 2. - Formation of Oxygenated Products," J. Chem. Soc., Faraday Trans. I, v 71, p 756 (1975).

42. Slagle, I.R., Park, J.Y. and Gutman, D., "Experimental Investigation of the Kinetics and Mechanism of the Reaction of n-Propyl Radicals with Molecular Oxygen from 297 to $635K$," Twentieth Symposium (International) on Combustion/The Combustion Institute, p 733 (1984).

43. Slagle, I.R., Ratajczak, E., Heaven, M.C., Gutman, D. and Wagner, A.F., "Kinetics of Polyatomic Free Radicals Produced by Laser Photolysis. 4. Study of the Equilibrium $i - C_3H_7 + O_2 = i - C_3H_7O_2$ between 592 and $692K$," J. Am. Chem. Soc., v 107, p 1838 (1985).

44. Lovell, W., "Knocking Characteristics of Hydrocarbons," Ind. Eng. Chem., v 40, p 2388 (1948).